HHS Public Access

Author manuscript

Anticancer Res. Author manuscript; available in PMC 2019 June 01.

Published in final edited form as:

Anticancer Res. 2018 June ; 38(6): 3299–3307. doi:10.21873/anticanres.12595.

Hapalindole H Induces Apoptosis as an Inhibitor of NF-κB and Affects the Intrinsic Mitochondrial Pathway in PC-3 Androgen-insensitive Prostate Cancer Cells

Ulyana Muñoz Acuña[1,2], **Shunyan Mo**[3], **Jiachen Zi**[3], **Jimmy Orjala**[3], and **Esperanza J. Carcache de Blanco**[1,2]

[1]Division of Pharmacy Practice and Administration, The Ohio State University, Columbus, OH, U.S.A

[2]Division of Medicinal Chemistry and Pharmacognosy, College of Pharmacy, The Ohio State University, Columbus, OH, U.S.A

[3]Department of Medicinal Chemistry and Pharmacognosy, College of Pharmacy, University of Illinois at Chicago, Chicago, IL, U.S.A

Abstract

Background—Prostate cancer presents the highest incidence rates among all cancer in men. Hapalindole H (Hap H), isolated from *Fischerella muscicola* (UTEX strain number LB1829) as part of our natural product anticancer drug discovery program, was found to be significantly active against prostate cancer cells

Materials and Methods—In this study, Hap H was tested for nuclear factor kappa-B (NF-κB) inhibition and selective cytotoxic activity against different cancer cell lines. Apoptotic effect was assessed on PC-3 prostate cancer cells by fluorescence-activated cell sorting analysis. The underlying mechanism that induced apoptosis was studied and the effect of Hap H on mitochondria was evaluated and characterized using western blot and flow cytometric analysis.

Results—Hap H was identified as a potent NF-κB inhibitor (0.76 μM) with selective cytotoxicity against the PC-3 prostate cancer cell line (0.02 μM). Apoptotic effect was studied on PC-3 cells. The results showed that treatment of PC-3 cells with Hap H reduced the formation of NAD(P)H, suggesting that the function of the outer mitochondrial membrane was negatively affected. Thus, the mitochondrial transmembrane potential was assessed in Hap H treated cells. The results showed that the outer mitochondrial membrane was disrupted as an increased amount of JC-1 monomers were detected in treated cells (78.3%) when compared to untreated cells (10.1%), also suggesting that a large number of treated cells went into an apoptotic state.

Conclusion—Hap H was found to have potent NF-κB p65-inhibitory activity and induced apoptosis through the intrinsic mitochondrial pathway in hormone-independent PC-3 prostate cancer cells.

Correspondence to: Dr. Esperanza Carcache de Blanco, 500 W. 12th Ave. Room 442, Columbus, OH 43210-1291, USA. Tel.: +1 6142477815, Fax: +1 6142921335, carcache-de-blan.1@osu.edu.

Keywords

prostate; mitochondria; apoptosis; inflammation; cancer; hapalindole H

Prostate cancer is a leading cause of cancer-related death for men and new therapeutic agents with fewer side-effects are needed to treat aggressive and metastatic prostate cancer types (1). Previous studies suggested that transcription factor nuclear factor-κB (NF-κB) plays a central role in regulating the expression of important regulatory factors and proteins involved in the metastasis of androgen-independent human prostate cancer cells PC-3 (2,3). The regulatory element and transcription factor NF-κB contributes to disease pathogenesis, and it has also been shown to prevent cancer cells from entering apoptosis (4). Tumor necrosis factor-α (TNF-α) plays a pivotal role in the activation of NF-κB in malignant diseases and in the metastasis of human hormone-insensitive cancer cells (5). In these cells, the TNF-α mediated activation of the NF-κB cell signaling pathway is responsible for tumor progression, cell growth, and metastasis (5,6). In addition, it has been suggested that NF-κB may induce expression of antioxidant genes, and exert protective effects against the damaging activity of reactive oxygen species (ROS) formed in the pathogenesis of cancer (7). Blockade of NF-κB has been found to suppress invasion and metastasis of prostate cancer cells (8). Furthermore, TNF-α induces NF-κB activity and promotes resistance to certain anti-tumorigenic agents (9). Thus, studying the effect of secondary metabolites from natural sources, such as cyanobacteria, on the NF-κB activating pathway in tumor cells, provides a unique approach for identifying new anticancer agents that selectively target cancer cells. A previous review reported that natural products display both high diversity in chemical scaffolds and biological activity against various types of cancer. It has been estimated that 60% of small molecules, including semi-synthetic derivatives in clinical use to treat cancer, derive from natural sources (10).

The aim of this study was to investigate the antiproliferative effects of hapalindole H (Hap H) (Figure 1) and its effects on mediators of the NF-κB pathway in hormone-independent PC-3 prostate cancer cells. The expression of the key mediators in the NF-κB pathway involved in the activation of subunit p65 were analyzed, as well as its effects in the activation of target proteins involved in cell adhesion and metastasis of prostate cancer cells.

Materials and Methods

Cells, media, and working reagents

Human cancer cell lines (PC-3, MCF-7 breast, and HT-29 colon cancer cells) were obtained from the American Type Culture Collection (Rockville, MD, USA). Dulbecco's modified Eagle's medium (DMEM), Roswell Park Memorial Institute medium (RPMI-1640), fetal bovine calf serum (FBS) and antibiotic-antimycotic supplement were obtained from Gibco (Rockville, MD, USA). Bradford protein assay kit, Supersignal Femto LumiGLO kit, human recombinant tumor necrosis factor-α (TNFα) and Transcription Assay System were obtained from Thermo Scientific (Rockford, IL, USA). Lithium dodecyl sulfate sample loading buffer (LDS), Nu-PAGE 10% SDS-PAGE Bis-Tris gel, SeeBlue® Plus2 Pre-Stained Standard Ladder, and Purelink RNase A were obtained from Invitrogen (Carlsbad, CA,

USA). Primary antibodies (anti-NF-κBp65 and p50, anti-IκB kinase (anti-IKKα), anti-IKKβ, intercellular adhesion molecule-1 (ICAM-1), and anti-caspase-3) were purchased from Cell Signaling Technologies (Beverly, MA, USA). Anti-rabbit horseradish peroxidase (HRP)-conjugated antibody was purchased from Santa Cruz Biotechnology, Inc. (Santa Cruz, CA, USA). $FeSO_4$ and tricholoroacetic acid (TCA) were obtained from Fischer Scientific (Fair Lawn, NJ, USA). Tris-buffered saline with Tween-20 buffer (TBS-T), vitamin C, propidium iodine (PI), 3,4-Dihydro-5-[4-(1-piperidinyl)butoxyl]-1(2H)-isoquinolinone (DPQ), Trizma® base, and fluorescent probe 2',7'-dichlorfluorescein-diacetate (DCFH-DA) were purchased from Sigma Aldrich (St. Louis, MO, USA). Sulforhodamine B, RNase A and 2,3-*bis*(2-methoxy-4-nitro-5-sulfophenyl)-2*H*-tetrazolium-5-carboxanilide (XTT) sodium salt were obtained from MP Biomedicals, LLC (Solon, OH, USA). Fluostar Optima plate reader was from BMG Labtech Inc, Durham, NC, USA.

Hapalindole H and reference compounds

The indole alkaloid Hap H was isolated from *Fischerella ambigua* as previously described (11). Reference compounds were obtained from different sources. Rocaglamide was purchased from Enzo Life Sciences, Inc. (Farmingdale, NY, USA). Daunorubicin was purchased from Tocris, Bristol, UK. Staurosporine was obtained from Cayman Chemical (Ann Arbour, MI, USA). Taxol was obtained from Tocris Bioscience, Bristol, UK. Hydrogen peroxide was obtained from Fluka Biochemika, Steinhiem, Switzerland.

Cell culture

The PC-3 androgen-insensitive human prostate, MCF-7 breast, and HT-29 colon cancer cells were cultured in DMEM and RPMI-1640 supplemented with 10% FBS and complemented with 10% antibiotic-antimycotic from Gibco. The cells were kept at 37°C and in a humidified atmosphere with 5% CO_2. The cells were grown to 80% confluency.

NF-κB assay

The NF-κB assay was performed according to established protocol (12). Tested samples were dissolved in dimethyl sulfoxide (DMSO). Nuclear extract from HeLa cells was evaluated using the Transcription Assay System (Pierce Biotechnology, Rockford, IL, USA). The assay was used to evaluate the binding affinity to biotinylated consensus sequence of the NF-κB subunit p65. Luminescence was detected using Fluostar Optima plate reader (BMG Labtech Inc,). Rocaglamide was used as a positive control.

SRB assay

Pre-cultured cells were suspended and seeded in 96-well microplates at a density of (5×10^4 cells/well). The cells were treated for 72 h with different concentrations of Hap H ranging from 2.75–55 μM (13). After incubation, cells were fixed using 20% TCA for 30 min. This step was followed by staining, using SRB (0.4%) for 30 min at room temperature. The SRB was removed with acetic acid (1%) then 200 μM Tris base solution was added to the wells and plates were placed on a shaker for 5 min. After shaking, the absorbance was read at 515

nm using Fluostar Optima plate reader (BMG Labtech Inc,). Paclitaxel was used as a positive control.

ROS assay

The assay was performed following a previously described procedure (14). The intracellular levels of ROS generated by Hap H were measured using a fluorescent probe, DCFH-DA. PC-3 cells were seeded in a 96-well plate and treated with Hap H (0.1–10 μM), followed by 5 h incubation at 37°C with 5% CO_2. Subsequently, cells were incubated with H_2O_2 (1.25 mM) and $FeSO_4$ (0.2 mM) for 30 min at 37°C. Afterward, the fluorescent probe DCFH-DA was added to determine intracellular ROS. Fluorescence was measured using a FLUOstar Optima fluorescence plate reader (BMG Labtechnologies Inc,) at an excitation wavelength of 485 nm and emission wavelength of 530 nm. All treatments were performed in triplicate and are representative of at least two different experiments.

Immunoblotting

To determine the effects of Hap H on the expression of mediators of the NF-κB pathway, cells were treated at five different concentrations (0.008, 0.016, 0.4, 2.0 and 10 μM) for 3 h at a temperature of 37°C and in an atmosphere containing 5% CO_2 (15). The cells were lysed using PhosphoSafe Lysis Buffer (Novagen). Protein concentration in the lysate was determined by using Bradford protein assay kit and albumin standard (Thermo Scientific). The absorbance was measured using Fluostar Optima plate reader (BMG Labtech GmbH, Inc.). Equal amounts of protein (20 μg) were loaded together with LDS sample loading buffer (Invitrogen) and resolved using Nu-PAGE 10% SDS-PAGE Bis-Tris gels together with SeeBlue® Plus2 Pre-Stained Standard (Invitrogen). Proteins were separated by electrophoresis and analyzed by western blot analysis with selected primary and secondary antibodies. The conjugated antibodies were detected using Chemiluminescent substrates, Supersignal Femto kit from Thermo Scientific, and relative band densities were determined.

PI staining and flow cytometry

Apoptosis was evaluated by fluorescence-activated cell sorting (FACS) analysis. Cells were plated and treated for 3 h using five different concentrations of Hap H, ranging from 0.0016 μM to 10 μM. After 3 h of incubation, cells were harvested and pelleted by centrifugation. Cells were then washed with ice-cold PBS and fixed with ethanol (70%). Prior to analysis, the cellular DNA was stained using 10 μg/ml PI solution in a reaction solution containing 1 mM EDTA and 100 μg/ml RNase A. The fluorescence emitted from the PI–DNA complex was quantified using BD FACS Canto II (BD Biosciences, San Jose, CA, USA) at 488 nm. In each analysis, 30,000 events were recorded.

Measurement of mitochondrial membrane potential (JC-1)

The status of the outer mitochondrial membrane potential (Ψm) was assessed using the JC-1 mitochondrial potential assay kit from Cayman Chemical Company (Ann Arbor, MI, USA) (16). The cytofluorimetric cationic dye 5,5',6,6'-tetrachloro-1,1',3,3'-tetraethyl-benzimidazolylcarbocyanine iodide (JC-1) was used to assess the ΔΨm. The selective dye changes color from green to red as the Ψm increases. Cells were seeded in plate before

being treated with Hap H (0.0016 μM) for 24 h. Thereafter, the cells were harvested using trypsin-EDTA from Gibco. Stain was added to the cells followed by incubation for 15 min at 37°C in 5% CO_2. Analysis was performed using BD FACS Canto II flow cytometer. Fluorescence was assessed using excitation wavelength of 520–570 nm and emission wavelength 570–610 nm, respectively.

XTT assay

To measure intracellular NAD(P)H using XTT assay, the protocol by Nakamura *et al.* was modified (17). Cells were seeded in a 96-well microplate and allowed to attach. Cells were then treated at different concentrations of Hap H and incubated at 37°C and 5% CO_2. Mitochondrial function was assessed by measuring the amount of formazan dye produced by metabolically active cells at 1-h intervals for over a period of 11 h. A solution containing 100 μl of XTT and 1-methoxy-5-methylphenazinium methyl sulfate was added to each well in DMEM to obtain final concentrations of 0.25 mM and 0.01 μM, respectively. The absorbance was measured at 485 nm and NAD(P)H depletion was calculated. Staurosporine (20 μM) was used as a positive control. Each sample was tested in triplicate in two independent experiments.

Results

Hap H, an indole alkaloid that contains a cyclized isoprene unit, was isolated from a cultured strain of cyanobacteria (blue-green algae) *Fischerella ambigua* (18–20). Hapalindole type alkaloids have been found to display antimicrobial and antifungal activity (21–25). However, in this study Hap H was found to be a potent inhibitor of NF-κB (50% inhibitory concentration, IC_{50}=0.76 μM) when tested using a luciferase assay, which measured the level of inhibition that Hap H had on the translocation of NF-κB into the nucleus (21–25).

Hap H also exhibited cytotoxic effects against different cancer cell lines: HT-29 colon cancer: 50% effective concentration (EC_{50}): =10.4 μM), MCF-7 hormone-dependent breast cancer: EC_{50}=5.96 μM, and the PC-3 hormone-independent prostate cancer cell line: EC_{50}=20 nM. The growth-inhibitory effect of Hap H on PC-3 cells was compared to that of the anticancer drug, paclitaxel (2.5 nM) (Figure 2) using the SRB assay. The inhibitory effect on cell viability for Hap H was 55.6% compared with 51.8% for paclitaxel when tested at the same concentration (2.5 nM). The cytotoxic effect of Hap H was also tested against CCD-112CoN cells, a normal colon cell line (data not shown), using taxol as a positive control. Hap H exhibited less than 50% inhibition at 100 μM (EC_{50} >20 μM). The fold selectivity ratio (FSR) was then calculated by dividing the EC_{50} value of the normal human colon cell line (CCD-112CoN) by the EC_{50} value for each cancer cell type, leading to FSR >1000 for PC-3 cells, FSR>3.35 for MCF-7 cells, and FSR>1.92 for HT-29 cells. The combination of both significant NF-κB-inhibitory and cytotoxic properties towards cancer cells, as well as the high FSR for PC-3 prostate cancer cells, suggested that NF-κB inhibition promoted apoptosis, and motivated preliminary mechanistic studies of Hap H as a potential natural product lead for anticancer drug development.

PC-3 cells were treated with Hap H at different concentrations and compared with the positive control, rocaglamide. Inhibitory effects on the NF-κB subunits p65 and p50 were

observed to occur in a dose-dependent manner (Figure 3A). Down-regulation in a concentration-dependent fashion of both of the regulating kinases, IKKα and IKKβ, was also observed (Figure 3B). The results showed that Hap H inhibited the upstream NF-κB pathway. Moreover, the adhesion molecule ICAM-1 was down-regulated in Hap H-treated cells (Figure 4). ICAM-1 is involved in the adhesion of cancer cells and the results suggest that NF-κB inhibition may contribute to preventing adhesion of PC-3 cancer cells.

Furthermore, after exposure of PC-3 cells to a high concentration of Hap H (10 μM) for 3 h, the percentage of viable PC-3 cells in the G_1-phase significantly decreased to 15.5% (Figure 5). Similar observations, discussed below, occurred at lower doses. This analysis suggested that the effect of Hap H on NF-κB inhibition induced apoptosis. Therefore, expression of caspase-3 (17 kDa) was evaluated (Figure 6). Caspase-3 expression decreased with increasing Hap H concentration, while that of procaspase-3 increased.

Hap H at the concentration used in this study also disrupted the outer mitochondrial membrane of treated cells. The percentage of JC-1 green fluorescent monomers detected in Hap H-treated cells was 78.3% compared with 10.1% in untreated cells (Figure 7). Meanwhile, the percentage of red JC-1 aggregates in the untreated cells was 69.3% compared with 10.1% in treated cells. These findings show significant disruption of the mitochondrial membrane and further analysis of the status of mitochondria was pursued using an XTT assay (Figure 8). Changes in the level of NAD(P)H in PC-3 cells were detected by reduction of formazan dye when using the XTT assay and different doses of Hap H. The amount of NAD(P)H was determined at 30-min intervals over a period of 11 h. The results suggest that the level of NAD(P)H was significantly affected, with the most noteworthy effect observed during the first 5 h of treatment. Thus, it appears that NF-κB may also be involved in the regulation of mitochondrial activity of PC-3 cancer cells and might be associated with changes in the outer mitochondrial membrane.

Variations in NAD(P)H level have been correlated to an increase in ROS levels and DNA damage of cancer cells. The ROS-inducing effect of Hap H on PC-3 cells was assessed against vitamin C as a negative control and hydrogen peroxide as a positive control. The results showed that increasing concentrations of Hap H induced oxidative stress in PC-3 cells and increased the level of intracellular ROS (Figure 9).

Discussion

The significant NF-κB -inhibitory effect of Hap H in the luciferase assay suggests that Hap H is a potent NF-κB inhibitor. Hap H was found be cytotoxic towards three different cancer cell lines: HT-29 colon cancer cell, MCF-7 hormone-dependent breast cancer and the PC-3 hormone-independent prostate cancer cell line; however, the cytotoxic effect of Hap H was significantly greater against PC-3 cells. The growth-inhibitory effect of Hap H at 2.5 nM on PC-3 cells was comparable to that of the anticancer drug, paclitaxel at the same concentration (Figure 2). Further analysis of the selectivity of the antiproliferative potential of Hap H was performed using CCD-112CoN (ATCC® CRL-1541) normal colon cells. Hap H exhibited minimal effect against normal cells with less than 50% inhibition at 100 μM

(EC_{50} >20 μM) and the FSR for the different cancer cell lines suggests that Hap H displayed high selectivity towards PC-3 prostate cancer cells.

Previous reports have shown that PC-3 cells exhibit higher normoxic expression and a more complete hypoxic induction of pro-inflammatory molecules compared to other prostate cancer cells (26). We examined expression of the NF-κB subunits, p65 and p50, and activating kinases IKKα and IKKβ by immunoblotting techniques (Figure 3). The results confirmed the inhibitory effect on NF-κB subunit p65 and subunit p50 as well as the down-regulating effect on both of the regulating kinases, IKKα and IKKβ. Moreover, the expression and the inhibitory effect were concentration-dependent, confirming the results obtained earlier using the luciferase reporter assay. This suggested that Hap H may have an inhibitory effect upstream in the NF-κB pathway.

Cell adhesion molecules, such as ICAM-1, are involved in cell proliferation and play a significant role in cancer progression and metastasis of tumors (27). In this study, the expression of ICAM-1 was analyzed by western blot analysis as ICAM-1 has also been reported as a prominent target gene of the NF-κB signaling pathway (28). The results indicated that ICAM-1 was down-regulated in the Hap H-treated cells. This suggested that the downstream effect of NF-κB inhibition resulted in the down-regulation of ICAM-1 in PC-3 cells (Figure 4). In previous studies, it was shown that cells stimulated by the inflammatory cytokine TNF-α expressed increased amounts of ICAM-1 (29,30). PC-3 Prostate cancer cells, preferentially adhere to bone, in part as a result of the enhanced expression of adhesion molecules that facilitate attachment to human bone marrow cells (26,31). The results from our immunoblot analysis suggested that the NF-κB inhibitory effects of Hap H could potentially prevent prostate cancer cells from metastasizing. Such interference in the adhesion of cancer cells, during the metastasis stage of the disease would halt the progression of the disease and possibly even prevent tumor cells from entering a dormancy state in bone marrow and other distant organs.

The apoptotic effect of Hap H on PC-3 cells was evaluated by cell flow cytometry using PI staining. The results from FACS analysis suggest that Hap H negatively affected the cell population in G_1-phase as it decreased to 15.5% in treated cells. An increase in the population of apoptotic sub-G_1 phase cells was observed, and the effect was concentration-dependent (Figure 5). Thus, the results show that Hap H induced apoptosis of PC-3 cells. The underlying mechanism inducing apoptosis in PC-3 cells was further investigated. The expression of procaspase-3 (32 kDa) was found to increase with increasing concentration of Hap H, while that of caspase-3 (17 kDa) decreased (Figure 6).

The gate-keeping role of the outer membrane of the mitochondria was investigated in Hap H-treated PC-3 cells, particularly, because mitochondrial dysfunction appears to play a key role in preceding apoptosis in cancer cells. In particular, apoptosis is regulated by proteins associated with the outer mitochondrial membrane such as B-cell lymphoma 2 gene (BCL2) (32). The expression of BCL2 is also regulated by NF-κB (33). Thus, the effect of Hap H on the mitochondrial transmembrane potential (Ψm) in PC-3 cells was assessed using JC-1 fluorescent dye. In PC3 cells treated for 3 h with Hap H, there was a complete loss of JC-1 aggregate fluorescence, indicating that Hap H efficiently reduced the outer membrane

potential and induced mitochondrial depolarization. This suggested that Hap H induced cell death in PC-3 prostate cancer cells through the mitochondria-dependent apoptotic pathway.

NAD(P)H is produced by mitochondria, and is used in cellular processes such as DNA repair and in the cytosol for anaerobic respiration (17). In this study, the level of NAD(P)H was most significantly affected during the first 5 h of treatment when using the XTT assay (Figure 8). The positive control staurosporine and the negative control PARP-1 inhibitor DPQ were used for comparison with the effect of Hap H on PC-3 cells. In staurosporine-treated cells, a small increase in NAD(P)H was initially detected before the level decreased below that in non-treated cells. Similarly, in Hap H-treated cells, the level of NAD(P)H initially increased in the cytosolic pool before falling below the level in non-treated cells. This suggests that initially NAD(P)H was released into the intracellular pool, possibly because of the disruption of the outer mitochondrial membrane and an increased permeability of mitochondria to NAD(P)H.

Furthermore, the XTT assay allowed for assessment of both the role of NAD(P)H and of DNA repair in PC-3 cells. The study revealed that PARP-1 inhibition by DPQ significantly increased the level of NAD(P)H in PC-3 cells. This suggests that PARP-1 and DNA repair play a significant role in the maintenance of PC-3 cells. Moreover, this suggests that androgen-independent prostate cancer cells, such as PC-3, may be sensitive to combination therapy with both PARP-1 and NF-κB inhibitors. It is possible that the increase in ROS induced by Hap H may lead to increased DNA damage in cancer cells. Thus, in this study the formation of intracellular levels of ROS was evaluated. The results obtained from the ROS assay indicated that increasing concentration of Hap H induced oxidative stress and increased the level of intracellular ROS (Figure 9), which is consistent with the results obtained from the XTT assay regarding the changes in level of NAD(P)H in treated cells.

In the present study, the pro-survival mechanism of cancer cells, and in particular the role of NF-κB, was evaluated in PC-3 cells. The results suggest that the NF-κB-inhibitory effect of Hap H was associated with apoptosis in androgen-insensitive prostate cancer cells, and negatively affected the outer mitochondrial membrane potential. Similarly, NF-κB inhibition down-regulates adhesion molecules such as ICAM-1 involved in the spreading of cancer cells, suggesting that Hap H may not only induce apoptosis in tumor cells but also prevent the metastasis of prostate cancer cells (27, 28). The results of this study suggest that indole-alkaloid type compounds may sensitize prostate PC-3 cells to undergo caspase-3-independent apoptosis.

Thus, the development of indole-alkaloids as new NF-κB inhibitors might increase the efficacy of existing anticancer drugs and may also increase the susceptibility of prostate cancer cells to cytotoxic chemotherapeutic agents. Indole-alkaloids, therefore, represent lead structures for future drug development. One further step to be considered includes the pursuit of *in vivo* studies on this highly promising drug lead. As part of this project, attempts were made for *in vivo* studies, but lack of adequate solubility of Hap H limited the completion of the study. We hope to pursue this further for future *in vivo* studies. Due to the great potential of this type of compound, the gene clusters responsible for biosynthesis for the chlorinated tetracyclic isoprenylated alkaloid type compounds have already been

identified (18). Furthermore, total synthetic methods of complex indole alkaloid structures, such as hapalindole H and ambiguine I, have been reported in an attempt to optimize this type of compound (34).

Conclusion

The indole-alkaloid, Hap H displayed potent p65 NF-κB-inhibitory activity. It also induced apoptosis through the intrinsic mitochondrial pathway in the PC-3 hormone-independent prostate cancer cell line. Thus, indole alkaloids with NF-κB inhibitory effect may have selective antiproliferative effects on cancer cells and prevent the metastasis of prostate cancer. They may also provide future lead structures for new antineoplastic agents.

Acknowledgments

The Authors greatly acknowledge the financial support through the program project grant P01CA125066 and the supplement P01CA125066-S1 from the National Cancer Institute, NIH, Bethesda, MD, USA to carry out the presented work.

References

1. Jemal A, Bray F, Center MM, Ferlay J, Ward E, Forman D. Global cancer statistics. CA Cancer J Clin. 2011; 61:69–90. [PubMed: 21296855]
2. Andela VB, Gordon AH, Zotalis G, Rosier RN, Goater JJ, Lewis GD, Schwarz EM, Puzas JE, O'Keefe RJ. NFkappaB: a pivotal transcription factor in prostate cancer metastasis to bone. Clin Orthop Relat Res. 2003:S75–85. [PubMed: 14600595]
3. Li J, Lai Y, Cao Y, Du T, Zeng L, Wang G, Chen X, Chen J, Yu Y, Zhang S, Zhang Y, Huang H, Guo Z. SHARPIN overexpression induces tumorigenesis in human prostate cancer LNCaP, DU145 and PC-3 cells *via* NF-κB/ERK/AKT signaling pathway. Med Oncol. 2015; 32:444. [PubMed: 25550157]
4. Darnell JE Jr. Transcription factors as targets for cancer therapy. Nat Rev Cancer. 2002; 2:740–749. [PubMed: 12360277]
5. Lerebours F, Vacher S, Andrieu C, Espie Marc, Marty M, Lidereau R, Bieche I. NF-kappa B genes have a major role in inflammatory breast cancer. BMC Cancer. 2008; 8:41. [PubMed: 18248671]
6. Yin Y, Chen X, Shu Y. Gene expression of the invasive phenotype of TNF-alpha-treated MCF-7 cells. Biomed Pharmacother. 2009; 63:421–428. [PubMed: 19564093]
7. Andela VB, Schwarz EM, O'Keefe RJ, Puzas EJ, Rosenblatt JD, Rosier RN. A genome-wide expression profile and system-level integration of nuclear factor kappa B-regulated genes reveals fundamental metabolic adaptations during cell growth and survival. FEBS Lett. 2005; 579:6814–6820. [PubMed: 16330031]
8. Huang S, Pettaway CA, Uehara H, Bucana CD, Fidler IJ. Blockade of NF-kappaB activity in human prostate cancer cells is associated with suppression of angiogenesis, invasion, and metastasis. Oncogene. 2001; 20:4188–4197. [PubMed: 11464285]
9. Sen GS, Mohanty S, Hossain DM, Bhatacharya S, Banerjee S, Chakraborty J, Saha S, a P, Batacharjee P, Mandal D, Bhatacharya A, Chattopadhyay S, as T, Sa G. Curcumin enhances the efficacy of chemotherapy by tailoring p65NFkappaB-p300 cross-talk in favor of p53-p300 in breast cancer. J Biol Chem. 2011; 286:42232–42247. [PubMed: 22013068]
10. Cragg GM, Grothaus PG, Newman DJ. Impact of natural products on developing new anti-cancer agents. Chem Rev. 2009; 109:3012–3043. [PubMed: 19422222]
11. Mo S, Krunic A, Chlipala G, Orjala J. Antimicrobial ambiguine isonitriles from the cyanobacterium Fischerella ambigua. J Nat Prod. 2009; 72:894–899. [PubMed: 19371071]
12. Deng Y, Balunas MJ, Kim J-A, Lantvit DD, Chin YW, Chai H, Sugiarso S, Kardono LB, Fong HH, Pezzuto JM, Swanson SM, Carcache de Blanco EJ, Kinghorn AD. Bioactive 5, 6-dihydro-α-pyrone derivatives from Hyptis brevipes. J Nat Prod. 2009; 72:1165–1169. [PubMed: 19422206]

13. Pan L, Kardono LBS, Riswan S, Heebyung C, Carcache de Blanco EJ, Pannell CM, Soejarto DD, McCloud TG, Newman DJ, Kinghorn AD. Isolation and characterization of minor analogues of silvestrol and other constituents from a large-scale re-collection of *Aglaia foveolata*. J Nat Prod. 2010; 73:1873–1878. [PubMed: 20939540]
14. Kim J-A, Lau EK, Pan L, Carcache de Blanco EJ. NF-κB inhibitors from *Brucea javanica* exhibiting intracellular effects on reactive oxygen species. Anticancer Res. 2010; 30:3295–3300. [PubMed: 20944100]
15. Acuna UM, Wittwer J, Ayers S, Pearce CJ, Oberlies NH, Carcache de Blanco EJ. Effects of (5Z)-7-oxozeaenol on MDA-MB-231 breast cancer cells. Anticancer Res. 2012; 32:2415–2421. [PubMed: 22753698]
16. Acuña UM, Matthew S, Pan L, Kinghorn AD, Swanson SM, Carcache de Blanco EJ. Apoptosis induction by 13-acetoxyrolandrolide through the mitochondrial intrinsic pathway. Phytother Res. 2014; 28:1045–1053. [PubMed: 24338805]
17. Nakamura J, Asakura S, Hester SD, Murcia G, Caldecott KW, Swenberg JA. Quantitation of intracellular NAD(P)H can monitor an imbalance of DNA single-strand break repair in base excision repair deficient cells in real time. Nucleic Acids Res. 2003; 31:e104–e. [PubMed: 12930978]
18. Micallef ML, Sharma D, Bunn BM, Gerwick L, Viswanathan R, Moffitt MC. Comparative analysis of hapalindole, ambiguine and welwitindolinone gene clusters and reconstitution of indole-isonitrile biosynthesis from cyanobacteria. BMC Microbiol. 2014; 14:213. [PubMed: 25198896]
19. Moore RE, Cheuk C, Patterson GML. Hapalindoles: new alkaloids from the blue-green alga Hapalosiphon fontinalis. JACS. 1984; 106:6456–6457.
20. Mo S, Krunic A, Chlipala G, Orjala J. Antimicrobial ambiguine isonitriles from the cyanobacterium Fischerella ambigua. J Nat Prod. 2009; 72:894–899. [PubMed: 19371071]
21. Shenvi RA, O'Malley DP, Baran PS. Chemoselectivity: the mother of invention in total synthesis. Acc Chem Res. 2009; 42:530–541. [PubMed: 19182997]
22. Klein D, Daloze D, Braekman JC, Hofmann L, Demoulin V. New hapalindoles from the cyanophyte Hapalosiphon laingii. J Nat Prod. 1995; 58:1781–1785.
23. Acuña UM, Zi J, Orjala J, Carcache de Blanco EJ. Ambiguine I isonitrile from Fischerella ambigua induces caspase-independent cell death in MCF-7 hormone dependent breast cancer cells. Intern J Cancer Res. 2015; 49:1655.
24. Raveh A, Carmeli S. Antimicrobial ambiguines from the cyanobacterium Fischerella sp. collected in Israel. J Nat Prod. 2007; 70:196–201. [PubMed: 17315959]
25. Ravenna L, Principessa L, Verdina A, Salvatori L, usso MA, Petrangeli E. Distinct phenotypes of human prostate cancer cells associate with different adaptation to hypoxia and pro-inflammatory gene expression. PloS One. 2014; 9:e96250. [PubMed: 24801981]
26. Haraldsen G, Kvale D, Lien B, Farstad IN, Brandtzaeg P. Cytokine-regulated expression of E-selectin, intercellular adhesion molecule-1 (ICAM-1), and vascular cell adhesion molecule-1 (VCAM-1) in human microvascular endothelial cells. J Immunol. 1996; 156:2558–2565. [PubMed: 8786319]
27. Rokhlin OW, Cohen MB. Expression of cellular adhesion molecules on human prostate tumor cell lines. Prostate. 1995; 26:205–212. [PubMed: 7536326]
28. Hoesel B, Schmid JA. The complexity of NF-κB signaling in inflammation and cancer. Molec Cancer. 2013; 12:86. [PubMed: 23915189]
29. Khatib A-M, Kontogiannea M, Fallavollita L, Jamison B, Meterissian S, Brodt P. Rapid induction of cytokine and E-selectin expression in the liver in response to metastatic tumor cells. Cancer Res. 1999; 59:1356–1361. [PubMed: 10096570]
30. Cohen MC, Bereta M, Bereta J. Effect of cytokines on tumour cell-endothelial interactions. Indian J Biochem Biophys. 1997; 34:199–204. [PubMed: 9343951]
31. Yanase M, Tsukamoto T, Kumamoto Y. Investigative urology: cytokines modulate *in vitro* invasiveness of renal cell carcinoma cells through action on the process of cell attachment to endothelial cells. J Urol. 1995; 153:844–848. [PubMed: 7532240]

32. Thapa D, Lee JS, Park M-A, Cho M-Y, Park Y-J, Choi H-G, Jeong T-C, Kim J-A. Inhibitory effects of clotrimazole on TNF-α-induced adhesion molecule expression and angiogenesis. Arch Pharmacol Res. 2009; 32:593–603.

33. Choi BT, Cheong J, Choi YH. β-Lapachone-induced apoptosis is associated with activation of caspase-3 and inactivation of NF-κB in human colon cancer HCT-116 cells. Anti-cancer Drugs. 2003; 14:845–850. [PubMed: 14597880]

34. Maimone TJ, Ishihara Y, Baran PS. Scalable total syntheses of (−)-hapalindole U and (+)-ambiguine H. Tetrahedron. 2015; 71:3652–3665. [PubMed: 25983347]

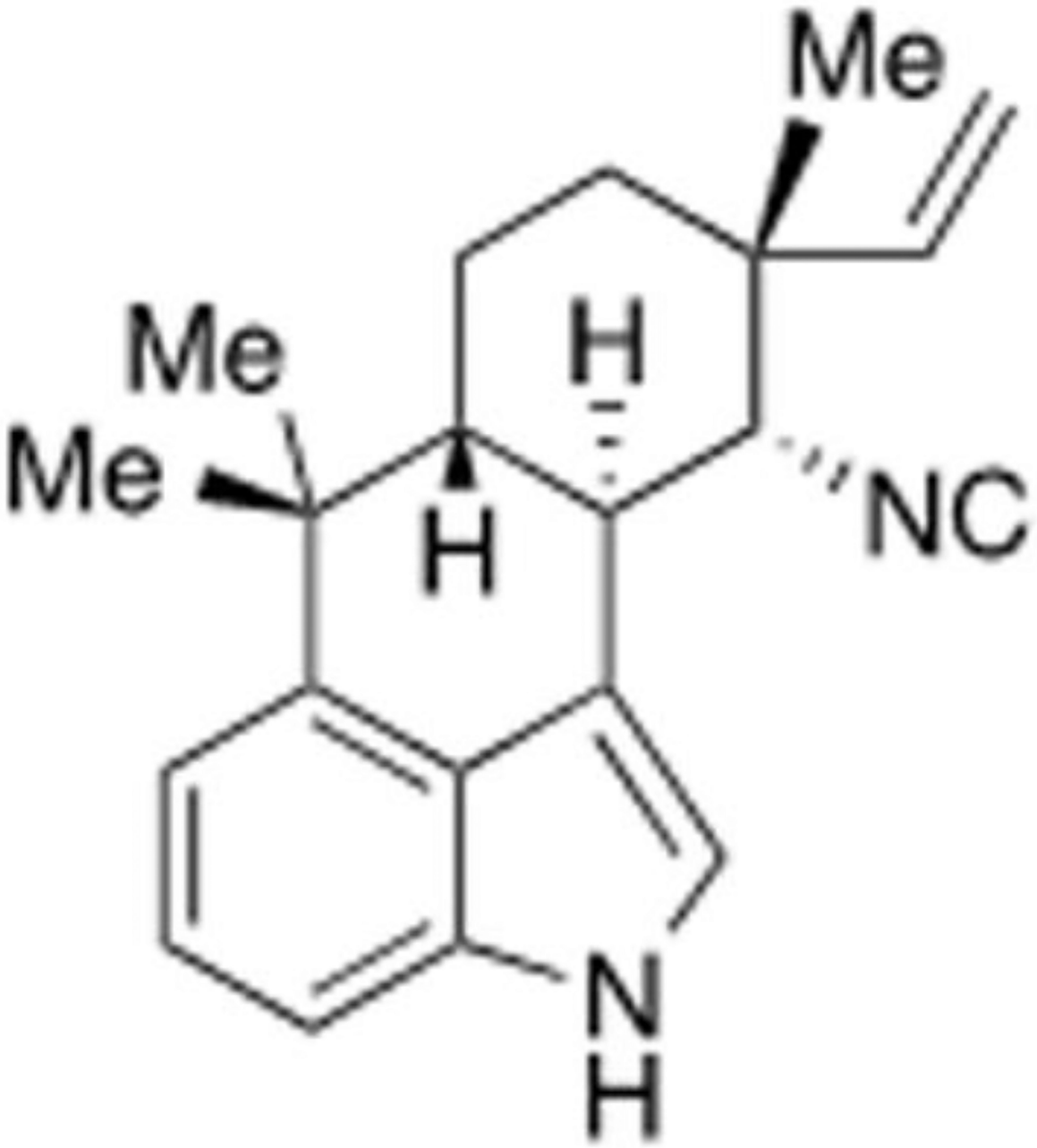

Figure 1.
Hapalindole H isolated from cyanobacteria *Fischerella ambigua*.

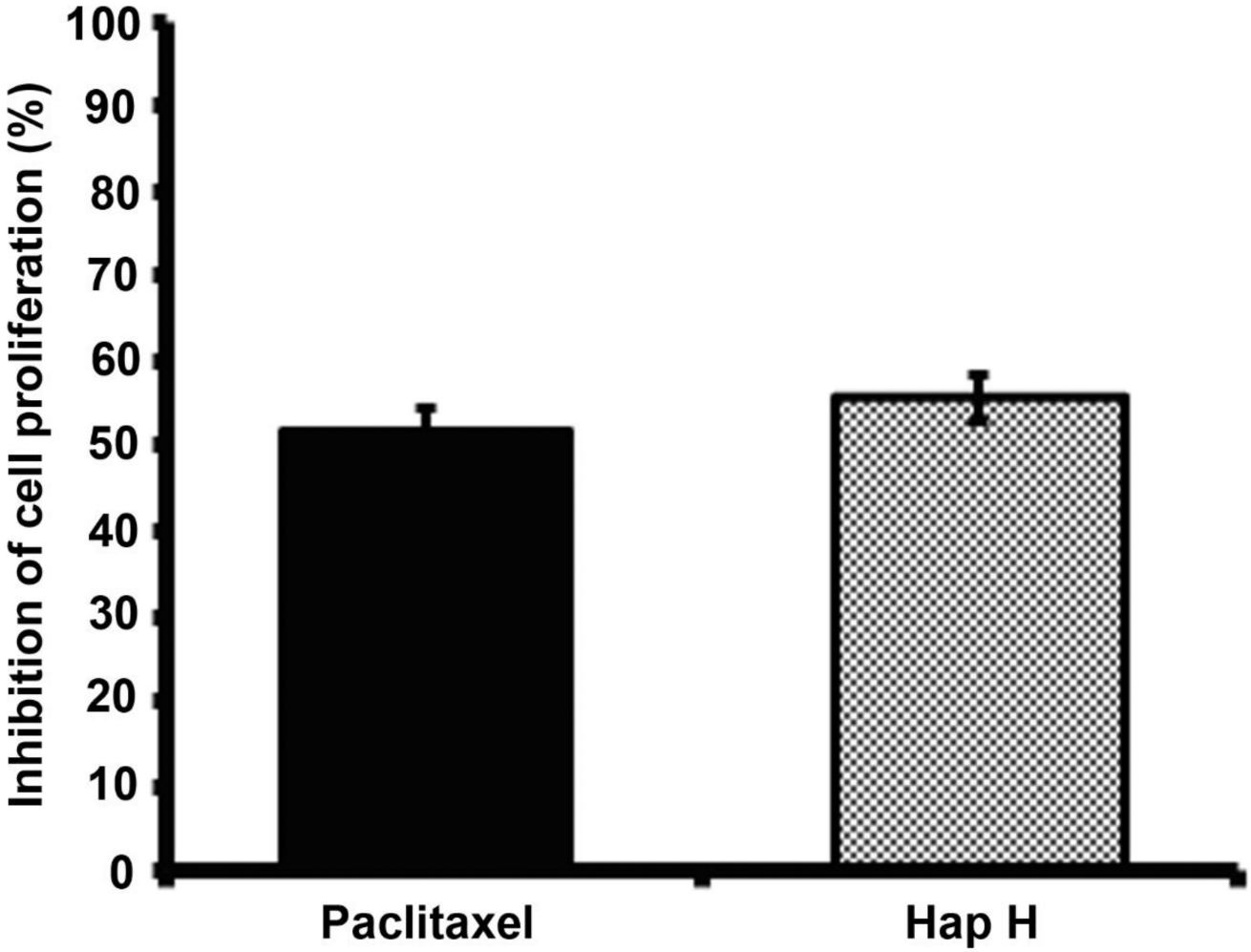

Figure 2.

The effect of hapalindole H (Hap H) on viability of PC3 prostate cancer cells after 72 h of treatment. The cytotoxic effect of Hap H on PC-3 cells was compared to the effect of paclitaxel at the same concentration (2.5 nM) and in triplicates. Values represent the means ± SEM from experiments. Student *t-test* showed $p>0.05$ when comparing paclitaxel vs. Hap H, suggesting Hap H as a lead structure for further development.

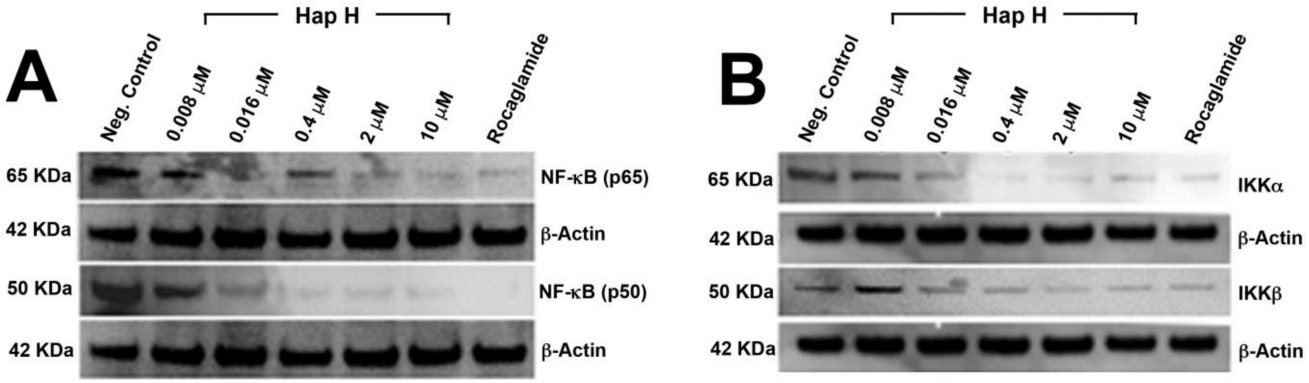

Figure 3.

Expression of nuclear factor kappa-B (NF-κB) subunits p65 and p50 (A) and mediators of the NF-κB pathway, IκB kinase alpha (IKK-α) and IKK-β, (B) in hapalindole H (Hap H)-treated PC-3 cells. Rocaglamide was used as a positive control.

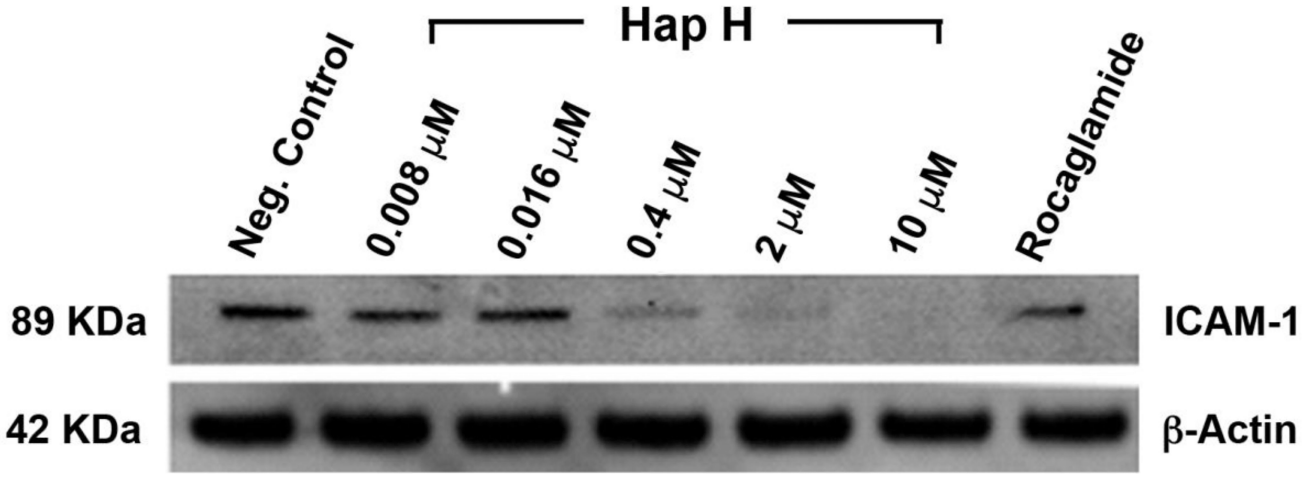

Figure 4.
Expression of intercellular adhesion molecule 1 (ICAM-1) in hapalindole H (Hap H)-treated PC-3 cells.

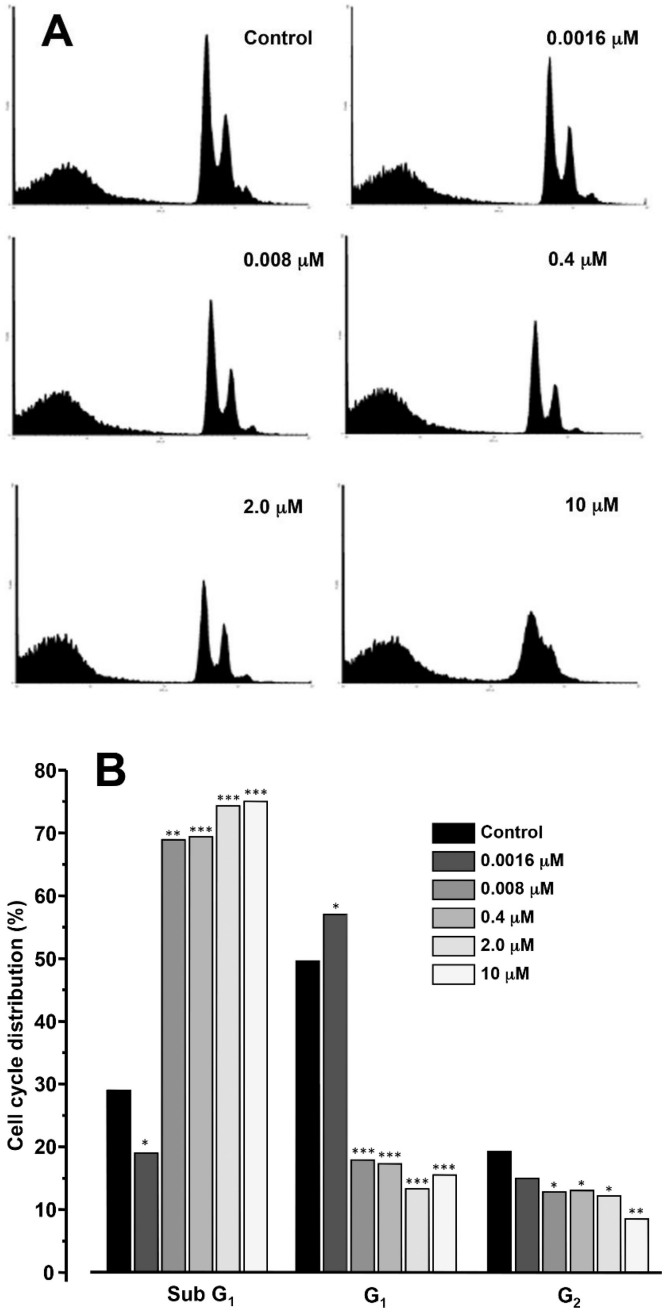

Figure 5.

Fluorescence-activated cell sorted flow cytometric (FACS) analysis of PC-3 cells treated with hapalindole H (Hap H) for 12 h. **A:** FACS histogram of control and hapalindole H (Hap H)-treated PC-3 cells. **B:** Bar graph of FACS data, suggesting that the apoptotic effect was concentration-dependent. Significant difference vs. control was observed at *p<0.05, **p<0.01 and ***p<0.001.

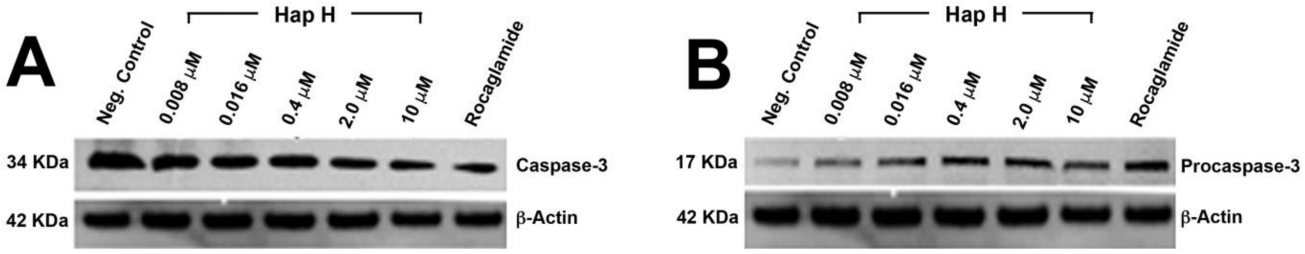

Figure 6.

Expression of caspase-3 (A) and procaspase-3 (B) in hapalindole H (Hap H)-treated PC-3 cells.

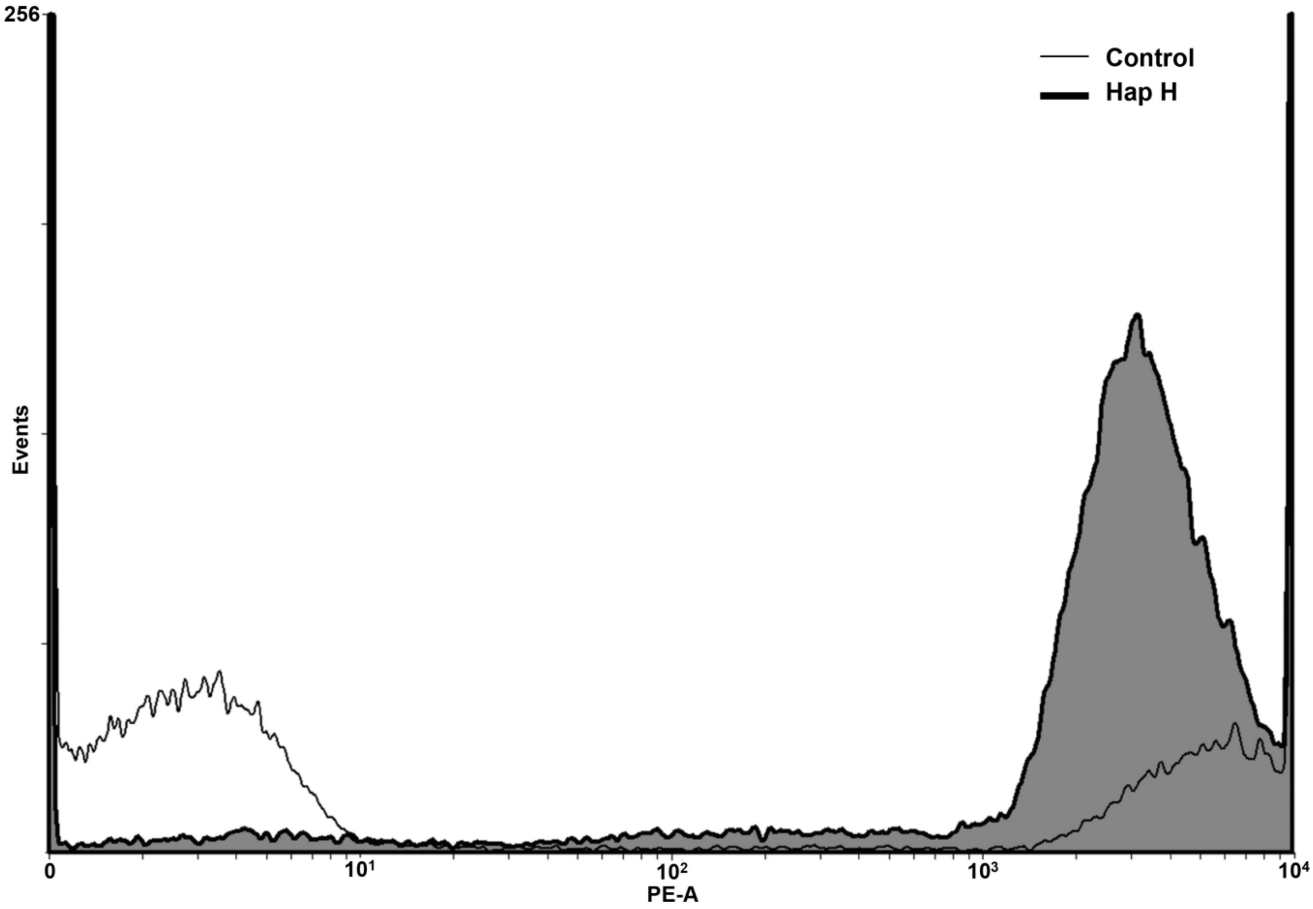

Figure 7.

The biochemical changes of the outer mitochondrial membrane potential was assessed in PC-3 hormone-independent prostate cancer cells after treatment with hapalindole H (Hap H). The amounts of JC-1 monomers and aggregates were determined in treated and untreated cells. The amount of JC-1 monomers detected in treated cells was higher (78.3%) compared to untreated cells (10.1%). This indicated that the outer membrane potential in Hap H-treated PC-3 cells was negatively affected and disrupted. JC-1 aggregates were detected at a higher level in the untreated cells (69.3%) compared to treated cells (10.1%). This confirmed that the treated cells had a disrupted outer mitochondrial membrane potential.

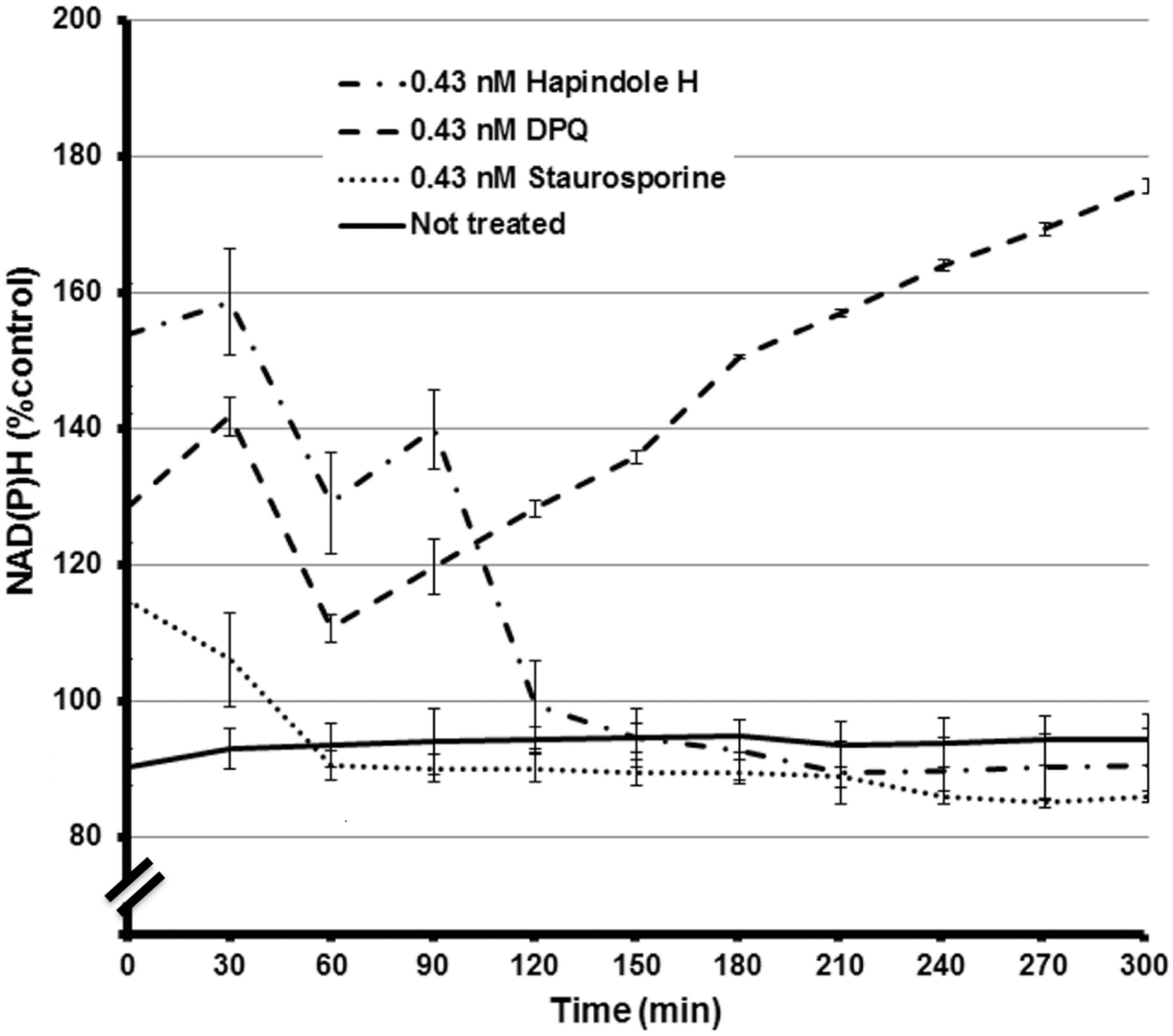

Figure 8.

Real-time assessment of the level of NAD(P)H in hapalindole H (Hap H)-treated and untreated PC-3 hormone-independent prostate cancer cells by XTT assay. Staurosporine and poly(ADP-ribose) polymerase 1 (PARP-1) inhibitor 3,4-dihydro-5-[4-(1-piperidinyl)butoxyl]-1(*2H*)-isoquinolinone (DPQ) were used as positive and negative controls, respectively. NAD(P)H is a substrate of PARP-1. Imbalance in the levels of NAD(P)H were detected during the initial 60 min for all treatments when compared with untreated cells. Comparison with the DPQ-treated cells suggests that reduction in NAD(P)H was due to a reduction in mitochondrial function and confirm the data collected from the mitochondrial membrane potential assay shown in Figure 7

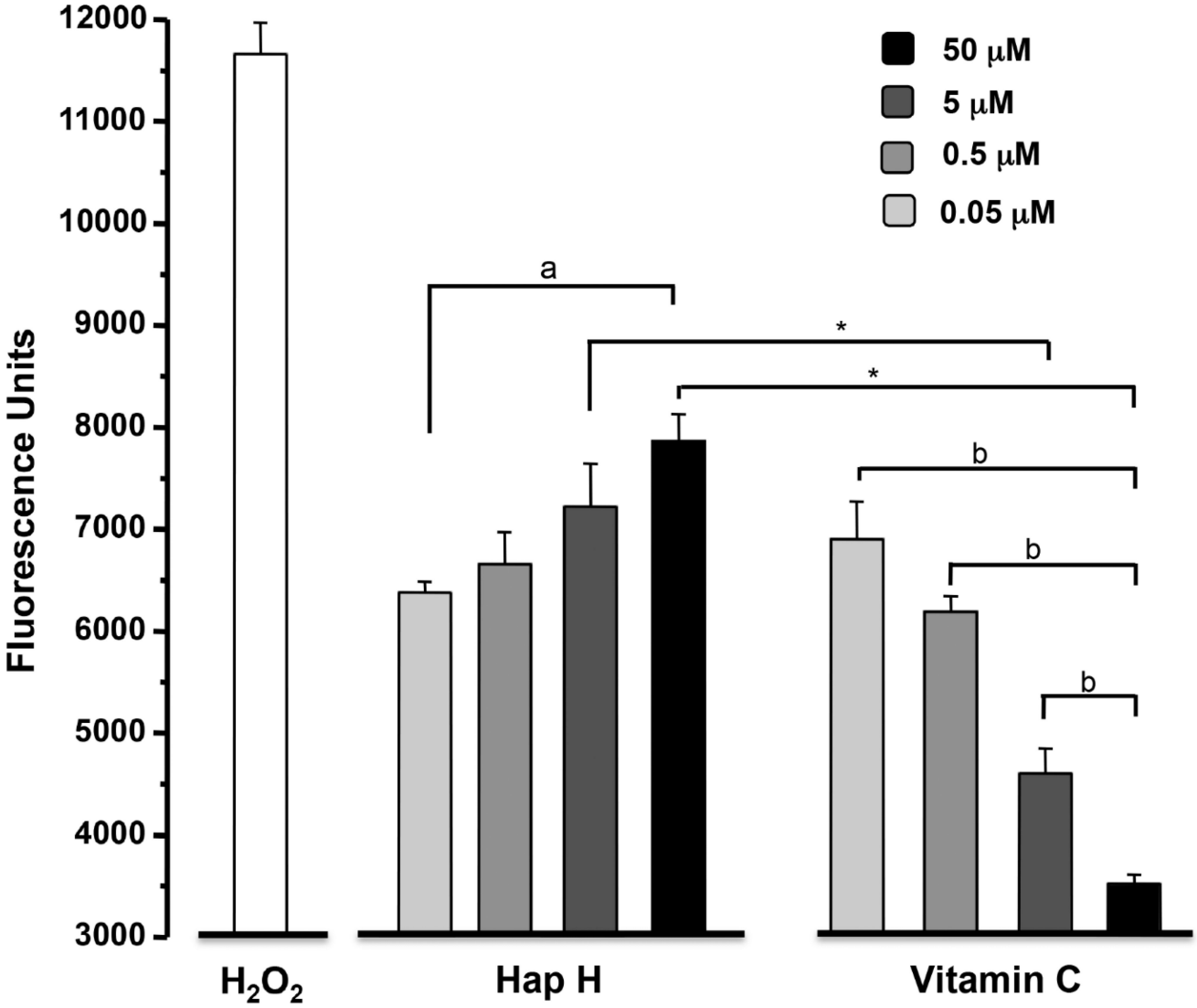

Figure 9.

Evaluation of oxidative stress by analysis of reactive oxygen species generated in hapalindole H (Hap H)-treated PC-3 cells. The negative control used was vitamin C and the positive control was hydrogen peroxide (H_2O_2). Statistical significance was determined using. Significantly different at: a: $p<0.05$ and b: $p<0.001$, one-way ANOVA; *$p<0.001$ by Student's *t*-test.